Influence of an Atmospheric Environment on the Fatigue Crack Growth Behaviour of the 8090 Aluminium-lithium Alloy

C. GOUNET LESPINASSE and C. BATHIAS
Mechanical Department- U.A. 849 du CNRS Université de Technologie de Compèigne, BP 649-Compiègne Cedex, France

ABSTRACT

The fatigue crack growth (FCG) resistance of the 8090 Al-Li-Cu-Mg-Zr alloy was investigated in humid air and in dry argon. Results were compared with those of the 7075 T651 high strength aluminium alloy.

The 8090 alloy exhibits good FCG behaviour. In humid air at low crack growth rates, the embrittling effect of the water vapour is emphasized and the effectiveness of roughness induced crack closure is discussed.

KEYWORDS

Aluminium-lithium alloy; Fatigue crack growth; Roughness induced crack closure; Fractography.

INTRODUCTION

It is well known that the addition of lithium results both in a density reduction and an elastic modulus increase. These properties are attractive for industries in search of mass savings such as the aircraft industry. The microstructure of new complex aluminium-lithium has been extensively studied (Sanders and Starke (1981,1984); Baker *et al.*,1986) but few works on their fatigue crack growth resistance have been conducted.

In these past years many studies have been devoted to the influence of roughness induced crack closure on FCG properties (Ritchie and Suresh ,1982; Suresh, 1985; Zaiken and Ritchie, 1985). Some authors have mentioned that good FCG behaviour of Al-Li alloys can be due to a pronounced roughness crack closure effect at low crack growth rates (Tintillier *et al.*, 1987; Peters *et al.*, 1987) since these materials are subjected to planar slip with a very crystallographic fracture aspect.

EXPERIMENTAL PROCEDURE

Material

The 8090 alloy has been supplied by PECHINEY in the form of 13x100 mm^2 section extruded plates. The composition of the alloy is listed in table 1 and tensile properties in the L direction are given in table 2.

Table 1. Chemical composition of the material

Element	Li	Cu	Mg	Zr	Fe
Weight %	2,2-2,8	1,1-1,7	0,7-1,3	0,08-0,16	< 0,3

Table 2. Tensile properties for L orientation

	Yield Stress (MPa)	U.T.S. (MPa)	Elongation (A%)
8090 PA	512	548	4,74
8090 OA	430	499	9,9

The plates had been : /1/ solution treated at 535°C, /2/ quenched in cold water, /3/ stretched by 2%, /4/ artificially aged : 12H at 190°C and 24H at 190°C resulting respectively in a peak aged temper (PA) and an overaged temper (OA).

The alloy is highly textured. The grain size variation along the S direction is given in Fig. 1 (Khireddine *et al.*). Since LT specimens are used in this study, the crack propagates in grains located at more than 30 mm from the surface of the plate in the T direction.

FCG testing

FCG tests were conducted on 12mm thick compact CT tension specimens (W=75mm, B=12mm) machined in the LT orientation. A 10 mm thick CT specimen was used just for one test.

Tests were conducted using a sinusoidal waveform with a frequency of 20Hz. The crack length was monitored with an optical method. The relative humidity was typically 60%.

RESULTS

FCG resistance

A salient feature of FCG behaviour of the 8090 alloy tested in humid air can be observed in Fig. 2 and 3. Whatever the ageing treatment and the load ratio investigated, a plateau of nearly constant crack growth rates is visible at the medium range (below 10^{-5} mm/cycle).

There is no significant difference in crack growth rates for the 2 ageing treatments on the whole ΔK range (Fig. 4).

The role of the air humidity is emphasized in Fig. 5. In dry argon, there is no longer a plateau of crack growth rates and the threshold value is enhanced.
In Figure 3, the 8090 OA alloy compares well at intermediate and high crack growth rates with the conventional 7075 T651 (Tintillier *et al.*,1987) alloy for a load ratio R=0.1 and using the same CT specimen. But it must be noticed that the 7075 T651 alloy exhibits a higher threshold value than that of the 8090 alloy. However, the FCG behaviour at low crack growth rates of the 8090 OA alloy can be significantly improved using a 10 mm thick specimen as shown in Fig. 6. The average grain width along T and S directions increases about 11% when using a 10 mm thick specimen instead of a 12 mm one.

Fractographic aspects

Macroscopic views of fracture surfaces reveal an unusual form of the crack front. The reversed form of the crack front indicates that cracks propagate quicker at the surfaces. Observations made with an optical microscope of the surface of specimens in a L-T plane, reveal the presence of slip bands for crack growth rates higher than 10^{-5} mm/cycle.

A marked change in the fracture surfaces occurs at crack growth rates close to 10^{-5} mm/cycle for both ageing treatments. A darkened area can be observed on the optical macrograph in Fig. 7a for crack growth rates higher than 10^{-5} mm/cycle. In this region, small numerous debris are visible using scanning electron microscopy (SEM) (Fig. 7d).

The crack growth mechanisms appear to be different at high and low crack growth rates as shown in the micrographs Fig. 7b and c. It must be noticed that the fracture surface has a crystallographic aspect on both micrographs, but for crack growth rates higher than 10^{-5} mm/cycle larger facets are visible at mid-thickness of the specimen (Fig. 7c).

At very high crack growth rates and in the quasi-static fracture region, large secondary intergranular cracks are visible.

DISCUSSION

The change in fracture aspect at mid-thickness of the specimen occurs at crack growth rates close to 10^{-5} mm/cycle which roughly correspond for both ageing treatments to a stress intensity factor range of 10 MPa$\sqrt{m}$. The flow stress of the peak aged and the overaged alloy in the T direction is the same and equal to 336 MPa. The reverse plastic zone size in plane strain conditions can be calculated using the following relationship :

$$D = (1/12\,\pi)\,(\Delta K/\sigma_y)^2 = 25\ \mu m \qquad (1)$$

The grain width in the S direction given in Fig. 1, is between 25-45 µm, at mid-thickness of the specimen. Thus for ΔK=10MPa$\sqrt{m}$, the reverse plastic zone size is no longer contained in a single grain. This could explain the observed change of fracture modes.

The fine, shearable and coherent δ' precipitation in aluminium-lithium alloys induces a planar slip mode. This is obvious for underaged tempers but for overaged tempers, mechanisms of deformation are not assumed to be so planar. Khirredine *et al.* (1988a, b) have performed low cycle fatigue tests on peak aged and overaged 8090 alloys. For shorter lives and thus for higher imposed strains, the deformation occurs along slip bands for both alloys. At lower imposed strains, the deformation occurs in loose veins for the peak aged temper and is no longer localized for the overaged temper. Some authors have already compared LCF and FCG substructures in different materials such as Nickel based superalloys

(Clavel and Pineau,1982) or Cu-Al alloys (Saxena and Antolovich, 1975). To make realistic such a comparison, the Mc Clintock model (Mc Clintock *et al.*,1963) must be assumed : the FCG propagation results from the accumulation of low cycle fatigue damage in a process zone at the crack tip.

The LCF observations are consistent with the aspect of fracture surface of specimens tested in FCG. Firstly, slip bands have been observed for crack growth rates higher than 10^{-5} mm/cycle and for higher imposed strains. Secondly, the fracture modes seem to be less crystallographic at low crack growth rates when the deformation is assumed to occur in loose veins.

It must be noticed that the unusual form of the crack front results from the change in the yield stress value from the surface to the core of specimens. In isotropic materials, the plastic zone size is larger near the surface and the crack growth rate is thus lower there. In 12mm thick specimens, the crack propagates quicker at the surface because of the brittleness of the superficial layer of small grains.

Reducing the specimen thickness from 12 to 10 mm, significantly increases the threshold value of the 8090 OA alloy. Many authors have noticed that the threshold value increases with increasing grain size (Masounave and Bailon, 1976; Backlund and al, 1981). Masounave and Bailon (1976) have shown that a linear relationship exists between the threshold value and the grain size square root in ferritic steels. However, it is not known whether the effect of grain size is due to 1/ deviations of the crack front further from the most favourably stressed direction, 2/ an increase of the size of ligaments produced by the break-up of the crack front, 3/ additional effects due to crack closure.

To explain the difference in crack growth rates when removing the layer of small grains, the roughness crack closure can be invoked. Enhancing the average grain size induces a rougher surface since larger grains make possible higher crystallographic deflections at low crack growth rates. A more pronounced surface roughness may promote 1/ a geometrical closure effect, 2/ an oxide induced crack closure effect through a fretting phenomenon. Some results indicate that roughness induced crack closure is effective in the near threshold region. Tintillier *et al.* (1987) have observed oxide deposits at low crack growth rates using X ray analysis, on a specimen of the 8090 peak aged alloy tested in air. These authors suggest that the oxide is created by a fretting or a rubbing phenomenon.

It must be noticed that the deformation mechanisms are not assumed to be planar for the investigated tempers in the near threshold region so that larger grains do not necessarily result in a rougher surface. Moreover, no evidence for a fretting phenomenon has been established for crack growth rates lower than 10^{-5}mm/cycle in this present study. In these conditions, it is not possible to state positively that roughness induced crack closure effects the FCG resistance of the 8090 alloy in the near threshold region.

Peters *et al.* (1987) have observed on fracture surfaces of the 8090 alloy tested in air, darkened areas created by fretting for the medium crack growth rates range which corresponds directly to the plateau (10^{-6}<da/dN< 10^{-5}mm/c). These authors suggest that the plateau is a result of crack closure due to surface roughness and fretting debris. This statement is not consistent with the results of tests conducted in inert environments. If the roughness induced crack closure were the predominant feature at intermediate crack growth rates, then the FCG results would be better in humid air than in dry argon or vacuum. Instead, in inert environments the FCG behaviour is enhanced at low and intermediate crack growth rates, suggesting that water vapour is the predominant feature at this stage. Other results underline the fact that the plateau does not result directly from roughness induced

crack closure. Crack closure effects are expected to disappear at high load ratios. Tests have been conducted on the 8090 alloy in air for load ratios equal to 0.7 (Peters *et al.*, 1987) and 0.8 (Tintillier *et al.*, 1987) and the plateau is still present. Moreover, the plateau extent is larger than at lower load ratios. This must be related to the fact that high ratios make crack tip access easier for the water vapour.

CONCLUSIONS

The water vapour contained in air induces an embrittling effect at low crack growth rates on the FCG of the 8090 alloy.
The plateau of nearly constant crack growth rates results from an environmental effect and not from a roughness induced crack closure effect as suggested.
The change of the fracture aspect observed for both ageing tempers occurs when the reverse plastic zone size is no longer contained in a single grain for crack growth rates higher than 10^{-5} mm/cycle. Moreover a change in mechanisms of deformation from low to high growth rates has been observed and is consistent with observations made elsewhere in LCF tests at low and high imposed strains.
The role of texture is emphasized at low crack growth rates : the removal of the superficial layer of small grains enhances the threshold value. The effectiveness of roughness induced crack closure has not been established at low crack growth rates.

ACKNOWLEDGEMENT

The authors wish to thank A. Clerivet for helpful discussions.

REFERENCES

Backlund J., A.F. Blom and C.J. Beevers eds. (1981). *Fatigue thresholds, Vol 1.* Stockolm.
Baker C., P.J. Gregson, S.J. Harris and C.P. Peel eds (1986). *Aluminium-Lithium alloys III.* Institute of metals, London.
Clavel M. and A. Pineau (1982). *Mat. Sci. and Eng., 55*, 157-180.
Khireddine D., R. Rahouadj, M. Clavel. to be published in *Acta. Met.*
Khireddine D., R. Rahouadj, M. Clavel (1988 a). Congrès sur la plasticité, Grenoble.
Khireddine D., R. Rahouadj, M. Clavel (1988 b). *Scripta Met.*, 22, 167.
Mc Clintock F.A., D.C Drucker and J.J. Gilman eds. (1963). *Fracture of solids*, 65. New York.
Masounave J. and J-P. Bailon (1976). *Scripta Met., 10*, 165.
Peters M., V. Bachmann and K. Welpmann. *Al-Li IV conference proceedings*, SFM, 785, édition de Physique. Paris.
Ritchie R.O. and S. Suresh (1982). *Met. Trans., 13A*, 937.
Sanders T.H. and E.A. Starke eds (1981). *Aluminium-Lithium alloys*, TMS-AIME.
Sanders T.H. and E.A. Starke eds (1984). *Aluminium-Lithium alloys II*, TMS-AIME.
Saxena A. and S.D. Antolovich (1975). *Met. Trans., 6*, 1809.
Suresh S. (1985). *Met. Trans., 16A*, 249.
Tintillier R., H.S. Yang, N. Ranganathan and J. Petit (1987). *Al-Li IV conference proceedings*, SFM, 777, édition de Physique. Paris.
Zaiken E. and R.O. Ritchie (1985). *Mat. Sci. and Eng.*, 70, 151.

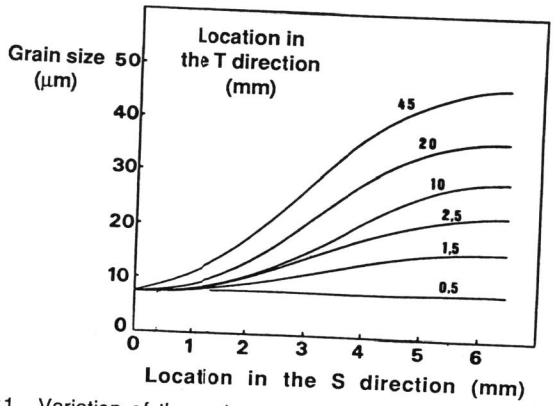

Fig. 1. Variation of the grain size in the S direction (Khireddine *et al.*).

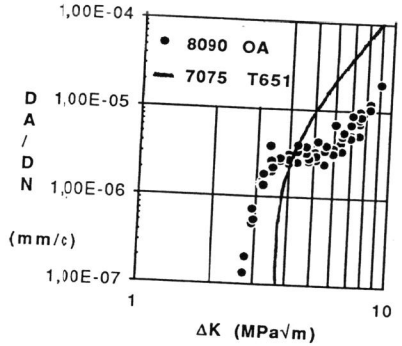

Fig. 2. FCG propagation of the 8090 OA and the 7075 T651 alloys (Tintillier et al., 1987) tested in LT orientations for R=0.1 in laboratory air.

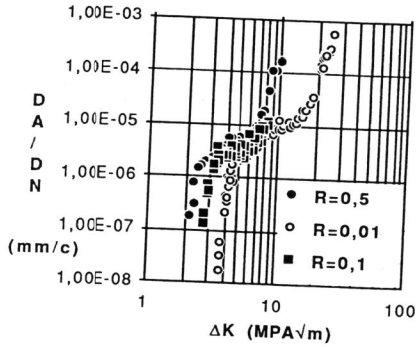

Fig. 3. Influence of the load ratio R on the FCG propagation of the 8090 OA alloy in laboratory air.

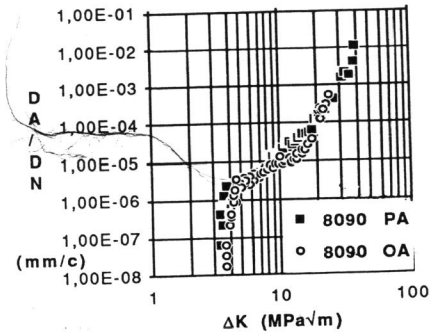

Fig. 4. Influence of the ageing treatment on the FCG propagation of the 8090 alloy for R=0.01 in laboratory air.

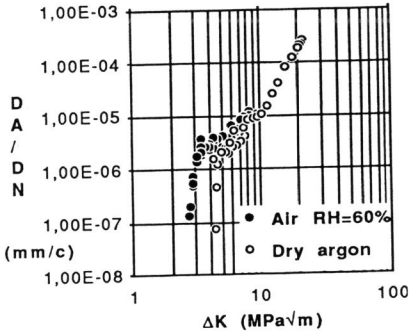

Fig. 5. FCG propagation of the 8090 OA alloy tested in laboratory air and in dry argon for R=0.1.

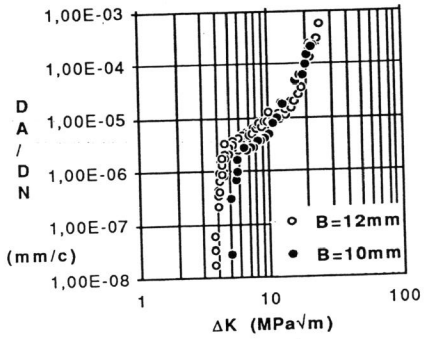

Fig. 6. FCG propagation of the 8090 OA alloy tested with 2 different specimen thicknesses for R=0.01 in laboratory air.

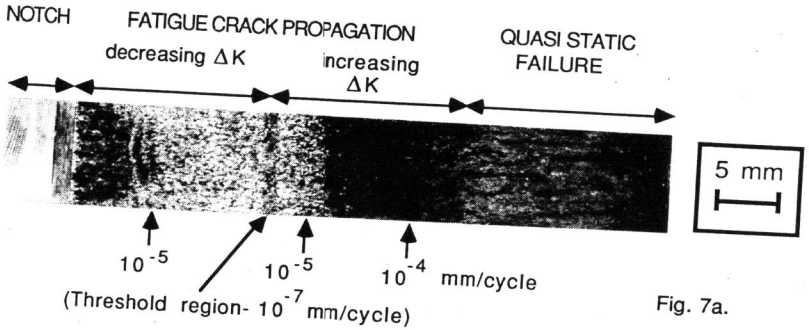

Fig. 7a.

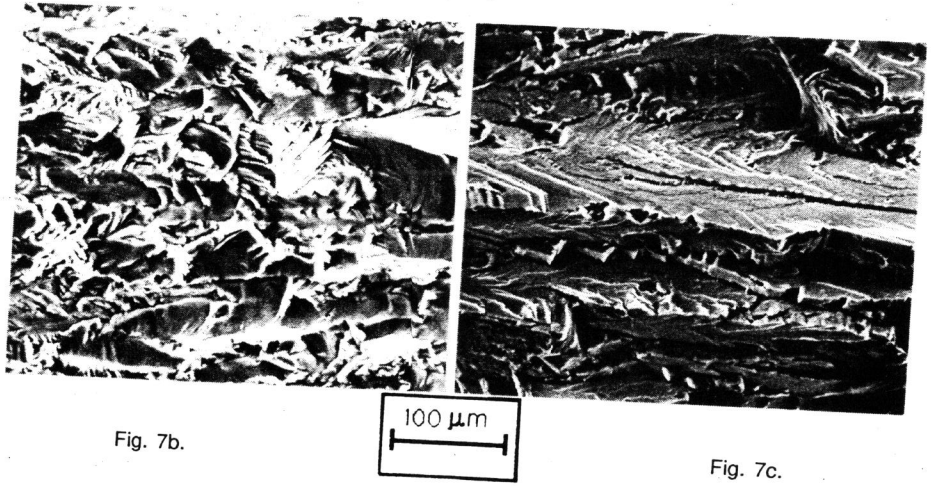

Fig. 7b.

Fig. 7c.

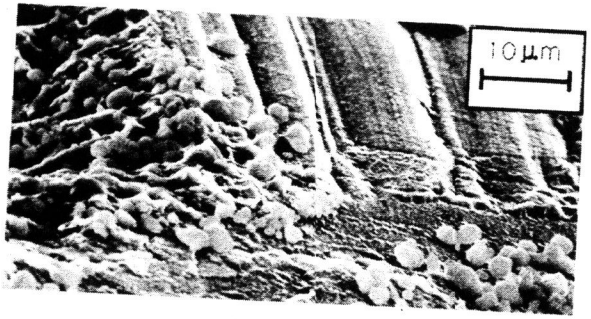

Fig. 7d.

Fig. 7. Fracture aspect of a CT specimen (B=10mm) of 8090 OA alloy tested in laboratory air.
a/ Macrograph of the specimen, b/ SEM micrograph- Threshold region, c/ SEM micrograph- Intermediate crack growth rate region, (10^{-5}mm/cycle), d/ SEM micrograph - Debris observed in the intermediate crack growth rate region.